Anisotropic Stretch-Induced Hypertrophy in Neonatal Ventricular Myocytes Micropatterned on Deformable Elastomers

Sindhu M. Gopalan,[1] Chris Flaim,[1] Sangeeta N. Bhatia,[1] Masahiko Hoshijima,[2] Ralph Knoell,[2] Kenneth R. Chien,[2] Jeffrey H. Omens,[1,2] Andrew D. McCulloch[1]

Departments of [1]Bioengineering and [2]Medicine, Whitaker Institute for Biomedical Engineering, University of California at San Diego, 9500 Gilman Drive, La Jolla, California 92093-0412, USA; telephone: 619-534-8102; fax: 858-534-0522; e-mail: jomens@ucsd.edu

Received 30 November 2001; accepted 22 July 2002

DOI: 10.1002/bit.10506

Abstract: Because cell shape and alignment, cell–matrix adhesion, and cell–cell contact can all affect growth, and because mechanical strains in vivo are multiaxial and anisotropic, we developed an in vitro system for engineering aligned, rod-shaped, neonatal cardiac myocyte cultures. Photolithographic and microfluidic techniques were used to micropattern extracellular matrices in parallel lines on deformable silicone elastomers. Confluent, elongated, aligned myocytes were produced by varying the micropattern line width and collagen density. An elliptical cell stretcher applied 2:1 anisotropic strain statically to the elastic substrate, with the axis of greatest stretch (10%) either parallel or transverse to the myofibrils. After 24 h, the principal strain parallel to myocytes did not significantly alter myofibril accumulation or expression of atrial natriuretic factor (ANF), connexin-43 (Cx-43), or *N*-cadherin (by indirect immunofluorescent antibody labeling and immunoblotting) compared with unstretched controls. In contrast, 10% transverse principal strain resulted in continuous staining of actin filaments (rhodamine phalloidin); increased immunofluorescent labeling of ANF, Cx-43, and *N*-cadherin; and upregulation of protein signal intensity by western blotting. By using microfabrication and microfluidics to control cell shape and alignment on an elastic substrate, we found greater effects for transverse than for longitudinal stretch in regulating sarcomere organization, hypertrophy, and cell-to-cell junctions. *Biotechnol Bioeng* **81**: 578–587, 2003.
Keywords: hypertrophy; micropatterning; microfluidics; neonatal cardiac myocytes; anisotropy

INTRODUCTION

Neonatal ventricular myocytes cultured on deformable silicone membranes have been used as an in vitro model for mechanical stretch-induced cardiac hypertrophy (Simpson et al., 1995). Cell shape and alignment, cell–matrix adhesion, and cell–cell contact can all affect cell growth and differentiation and are likely to modulate their responses to external forces. However, these factors are not normally controlled in neonatal cardiomyocyte cultures, nor are they typically representative of conditions in vivo. Cultured neonatal myocytes are randomly arrayed and multipolar when spread and adhered to an extracellular matrix immobilized on a surface, whereas they are rod-shaped and aligned in vivo. Mechanical strains in vivo are multiaxial and anisotropic, but previous in vitro stretch systems have been uniaxial or isotropic. The objective of this study was to develop an in vitro system for engineering neonatal cardiac myocytes so that cell shape and alignment, cell–matrix adhesion, and cell–cell contact could be independently controlled, and to investigate the effects of anisotropic mechanical strains on aligned rod-shaped cells.

External mechanical loading of myocytes can increase protein synthesis rates (Simpson et al., 1999), promote myofibrillogenesis and induce hypertrophy (Sadoshima and Izumo, 1993), accelerate connexin-43 expression and gap junction formation (Zhuang et al., 2000), and (if the load is too great) induce apoptosis (Anversa et al., 1986). Simpson et al. (1999) reported that the orientation of stretch applied to aligned myocytes affects the hypertrophic response. However, their method (Simpson et al., 1994a) for promoting polymerization of collagen into parallel fibrillar arrays on the culture surface could not be engineered to control independently cell shape and alignment or cell–cell contact nor to vary extracellular matrix concentration and composition. Therefore, we adopted a microfabrication technique using soft lithography and microfluidics (Bhatia et al., 1999; Delamarche et al., 1997; Desai et al., 2000; Deutsch et al., 2000) to achieve spatial control of cells cultured on elastic surfaces.

Photolithographic etching of glass substrates and immo-

Correspondence to: J. H. Omens

Contract grant sponsors: National Science Foundation; Procter and Gamble Co.; American Heart Association; National Institutes of Health; David and Lucile Packard Foundation

Contract grant numbers: BES-0086482; HL 43026; HL 46345

bilization of adhesive molecules have been used to control cell–surface interactions and to micropattern various cell types (Bhatia et al., 1997; Chen et al., 1997; Lom et al., 1993). Rohr et al. (1991) grew neonatal rat ventricular myocytes on photoetched glass to control cell shape, alignment, and contact for studying action potential propagation. Because soft elastomers are not suited to microlithography, we patterned extracellular matrix proteins onto silicone membranes using a microfluidic template with 10- to 100-μm channels constructed by replica-molding polydimethylsiloxane (PDMS) from a microfabricated silicon master. Matrix micropatterning and substrate surface treatments allowed parallel individual strands of aligned elongated myocytes to be grown. Micropatterned membranes were installed in a modification of our static equibiaxial stretch device (Lee et al., 1996; Summerour et al., 1998) with an elliptical indenter that applies homogeneous, anisotropic strain with respect to cell orientation.

Myocardial cells respond to changes in the mechanical forces imposed on them with changes in myocardial force development in the short term, and with structural remodeling in the long term. Actin is a major component of the cytoskeleton, and may be important for transmitting mechanical signals that activate the hypertrophic response to increased hemodynamic load (Wang and Ingber, 1994). It has also been shown that myocardial cells respond to mechanical load with changes in the distribution and number of gap junctions (Wang et al., 2000). Cell contact is an independent factor modulating cardiac myocyte hypertrophy and survival. Thus, in this study we examine the stretch response of the actin structures, gap junctional proteins connexin-43 and *N*-cadherin, and atrial natriuretic factor (ANF), which is a well-known indicator of myocyte hypertrophy.

MATERIALS AND METHODS

Photolithography and Replication Molding

Photolithographic patterning of silicon wafers was carried out as described previously (Bhatia et al., 1998) and is depicted schematically in Figure 1. Negative photoresist Epon SU8 was coated on a silicon wafer, exposed to ultraviolet light (365 nm) through a transparency mask, and developed using a modified method of Folch et al. (1999). Masks were generated by high-resolution printing of patterns with 10- to 100-μm parallel lines and 300-μm spacing. Using this technique, features >8 μm were reproducibly generated. Polydimethylsiloxane was prepared from a mixture of two liquid components (Sylgard 184 Kit, Dow Corning), poured onto the developed wafer, and cured. The resulting replicas were peeled off the master leaving deep microchannels with the specified width and separation. The ends of the mold were cut to expose the ends of the channels and the resultant channels were utilized as a microfluidic network to pattern the extracellular matrix (ECM) substrates.

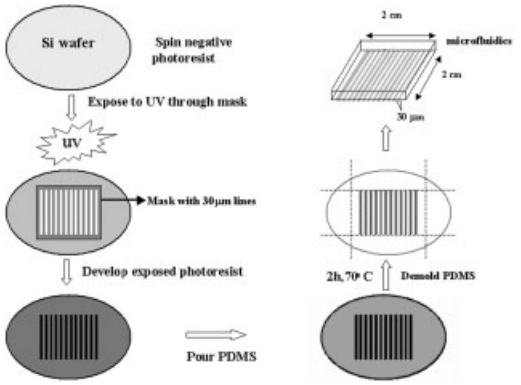

Figure 1. SU8 process and PDMS replication from the Si master. The Si wafer was spin-coated with SU8 and exposed to ultraviolet light through a mask with 30-μm lines. The micropatterns were developed on the Si master, and the master was covered with PDMS prepolymer. After curing, the PDMS mold was removed, and the edges cut off to expose the free edges of the channels. The final PDMS mold is about 2 cm^2.

Matrix Micropatterning on Silicone Elastomeric Membranes

The PDMS microchannel mold was sealed against a transparent silicone elastomeric membrane (0.25 mm thick, gloss finish; Speciality Manufacturing, Saginaw, MI) installed in a biaxial stretch device (see later) creating a seal between the mold and elastomer and leaving the microchannels open at both ends. Collagen solutions were prepared by dissolving 3 mg of type I collagen (Sigma Co., St. Louis, MO) in 1 mL of 0.1 *M* acetic acid and further diluted with sterile phosphate-buffered saline (PBS) to the desired concentration (10 to 3000 μg/mL). We typically placed 0.2 mL of collagen solution at one end of mold, and achieved continuous perfusion by applying a vacuum to the other end, producing uniform coverage. Using this method we could ensure that collagen coverage was uniform throughout the channel, which may not occur with capillary action (Delamarche et al., 1997). After all channels were completely filled with the solution, the assembly was placed an incubator at 37°C for 1 h to allow protein adsorption to the elastic substrate before the mold was carefully removed. To verify that this technique works with different extracellular matrix substrates, laminin, vitronectin, and fibronectin (Sigma) were also patterned onto silicone membranes. Immunofluorescent labeling and electron microscopy of these matrix proteins were done to confirm reproducible patterning (Fig. 2). As described in the next sections, studies were also carried out with neonatal cardiac myocytes grown only on the type I collagen patterns.

Surface Treatment

Pluronic F108 was used to produce a protein repellent coating between the matrix stripes on the silicone membrane. F108 (Spectrum Chemical Manufacturing Corp.) is a triblock polymer having polypropylene centers with polyethylene oxide side chains, and an average molecular weight of

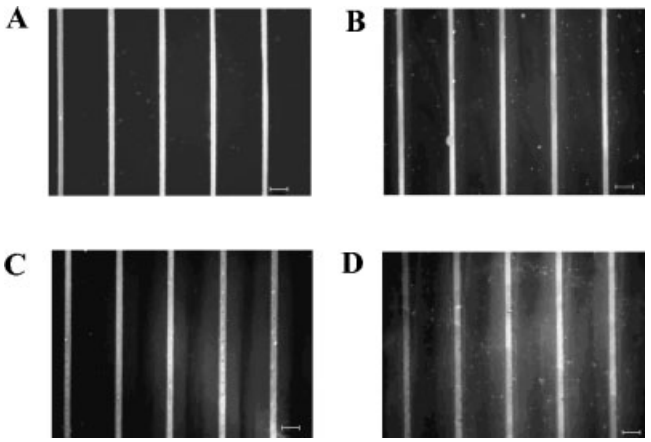

Figure 2. Indirect immunofluorescent antibody labeling of different ECMs patterned on silicone elastomers: (A) fluorescent collagen (conc. 1 mg/mL); (B) laminin; (C) fibronectin; and (D) vitronectin. Patterns were imaged by primary antibody labeling and detected with fluorescent secondary antibodies. Each of these ECM proteins produced excellent micropatterns on the elastomer. Vitronectin assay shows some nonspecific background adhesion. Scale bars = 100 μm.

17,000 g/mol. Polyethylene oxide (PEO) surface coating has been widely reported to repel protein and cell adhesion due its hydrophilicity, flexibility, chain mobility, and high steric exclusion volume in water (Jo and Park, 2000). Liu and co-workers demonstrated the utility of F108 to localize PEO in micropatterned systems using simple adsorption (Liu et al., 2002). Patterned silicone elastomers were exposed to 2% (w/w) solution of F108 in sterile PBS for 12 h at 37°C (Fig. 3).

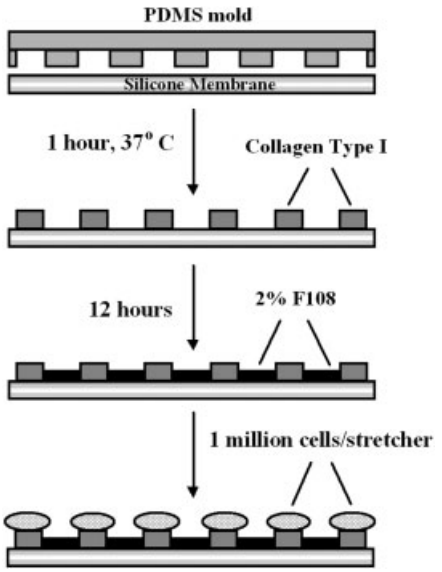

Figure 3. Schematic drawing of surface modifications to the silicone elastomer. Type I collagen is patterned on the silicone elastomer using the PDMS mold. Non-cell-adhesive moieties between the collagen patterns are produced by immobilizing Pluronic F108, a polyethylene oxide-terminated triblock polymer, to the silicone membrane. One million neonatal cardiac myocytes per stretcher are used to obtain patterned myocytes.

Measurement of Collagen Adsorption

The concentration of collagen I adsorbed on the patterned surfaces was estimated by radiolabeling using collagen (type I), *N*-[propionate-2-3-^{3}H] propionylate (NEN Life Science Products, Inc.), and unlabeled type I collagen in a fixed ratio, using a modification of the protocol described elsewhere (Chandy and Sharma, 1986; Liu et al., 2002; Uniyl and Brash, 1982). Tritiated collagen was patterned with concentrations ranging from 10 to 3000 μg/mL. Collagen mixture (0.2 mL) was used for each pattern, and a 2 × 2 cm^2 piece of elastic membrane was cut out, rinsed with PBS, incubated in a scintillation cocktail (EcoLume, ICN Biomedical), and analyzed for radioactivity by liquid scintillation counting (Rackbeta 1214, Wallac-LKB, Turku, Finland). These tests were carried out in triplicate for each concentration and then compared with measurements from unpatterned membranes. The collagen concentration was computed from $C_p \cdot R_b/(A \cdot R_s)$, where C_p is the concentration of collagen in the injecting solution, R_b is the count at the surface, A is the surface area, and R_s is the reference count per milliliter of collagen solution (Chandy and Sharma, 1986; Liu et al., 2002; Uniyl and Brash, 1982).

Anisotropic Cell Stretch

Silicone membranes were installed before matrix micropatterning in the anisotropic cell stretch device illustrated in Figure 4A and B. In a modification of a previously described equibiaxial stretcher (Lee et al., 1996), the polycarbonate indenter and membrane holder were elliptical instead of circular. The elastic membrane was clamped into an elliptical groove in the bottom of the membrane holder by a silicone rubber O-ring. The indenter ring was fit inside the membrane holder and pushed down by a flange when the screw top was turned. The resulting homogeneous strain field had a constant ratio of maximum-to-minimum principal stretching determined by the 2:1 ellipticity of the indenter, with the axis of maximum principal stretch being the minor axis of the ellipse. As in the original report (Lee et al., 1996), we confirmed that the new device applied homogeneous anisotropic two-dimensional strains both to the membrane and to adhered cells. To validate uniform membrane deformation, we used unpatterned membranes and calculated two-dimensional strains at five different locations on the membrane (based on displacements of sets of three closely spaced ink markers) for three different membranes (n = 15 total). The results were very consistent between membranes and location: the strain along the short axis of the ellipse was 0.108 ± 0.015 (range 0.126 to 0.088), and the strain along the long axis of the ellipse was 0.055 ± 0.013 (a strain of 0.105 is exactly equivalent to 10% stretch). Theoretically, the shear strain would be zero for this deformation and was found to be 0.014 ± 0.011. Thus, we found the strains to be homogeneous across the membrane, except within 2 mm of the indenter ring. Cell deformations were also verified in separate experiments with 1-μm fluorescent

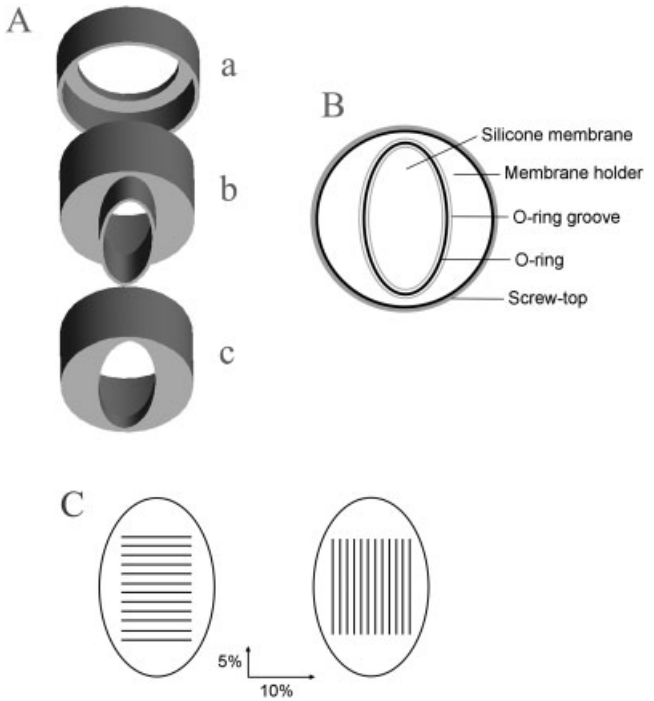

Figure 4. (A) Three-dimensional schematic representation of the elliptical stretching device for cultured cells, as modified from the equibiaxial approach of Lee et al. (1996). (a) Screw top, (b) indenter ring, and (c) membrane holder. Indentation of the membrane by the indenter ring applies homogeneous, anisotropic strain to the substrate and cultured cells. The magnitude of the strain is controlled precisely by the turns of the threaded screw top, which pushes the indenter ring onto the membrane. The elastic membrane is fixed to the membrane holder section with an O-ring as shown in (B). (C) Schematic representation of directional patterning of collagen on elliptical stretchers. In the configuration at left (horizontal lines), cells undergo 10% stretch along their short axis and 5% stretch along their longitudinal axis. In the configuration at right, cells undergo 10% longitudinal and 5% transverse stretch.

microspheres attached to the cells (Lee et al., 1996). We found cellular stretch to be within 10% of the membrane stretch.

Microfluidic templates were positioned so that the myocytes were aligned with either the major or minor axis of the ellipse. Anisotropic stretch was applied to the membranes to achieve maximal stretch of 10% in the minor axis direction and 5% in the major axis direction. Elongated cells on the patterned substrate were either stretched with 10% longitudinal (5% transverse) or 10% transverse (5% longitudinal) stretch, depending on the alignment of the pattern with the axes of the ellipse (Fig. 4C). Controls cells were grown in identical devices but not stretched.

Cell Culture

Primary neonatal ventricular myocytes from 1- to 2-day-old Sprague–Dawley rats were prepared using a standard Percoll gradient method as described previously (Iwaki et al., 1990). Myocytes were isolated and separated from fibroblasts by a selective attachment method (Borg et al., 1984). Cells were plated at a density of 1 million cells per stretcher. Each stretcher had an approximately 2-cm^2 surface area of micropatterned membrane. Cells were plated on the patterned elastomer in high-serum media containing Dulbecco's modified Eagle medium (DMEM), 3.8% M199, 3.8% horse serum, 2% fetal bovine serum (FBS), antibiotics (100 units/mL penicillin, 50 μg/mL streptomycin, 0.25 μg/mL amphotericin B), and cytosine. Twenty-four hours later, the media was changed to low-serum media containing 18.4% M199, 5.4% horse serum, and 1% FBS and antibiotics. All chemicals and media were obtained from Gibco (Grand Island, NY). Cells were maintained at 37°C in an atmosphere of 5% CO_2 in air. On the fourth day of plating, cells were stretched anisotropically and held with static stretch for 24 h before performing immunohistochemistry and cell harvesting for immunoblotting.

Adhesion Assay

Adhesion of neonatal cardiac myocytes to various concentrations (10 to 3000 μg/mL) of collagen substrate was assayed as described elsewhere (MacKenna et al., 1998). Myocytes were allowed to attach and align on the micropatterned channels. One day later, media was removed after gentle shaking to remove unattached cells and cells in between channels, then washed with PBS twice. Cells were fixed with 4% paraformaldehyde in PBS and stained overnight with 5 mg/mL crystal violet (Sigma) in 20% methanol. Stained cells were solubilized with 2% sodium dodecylsulfate (SDS) and absorbance was measured using a spectrophotometer (Beckman DU 640) at 590 nm. Percentage of cell adhesion was calculated from the absorbance of the SDS-solubilized solution of one million stained cells and total area of collagen pattern on each membrane.

Immunohistochemistry

Myocytes were cultured under the different loading conditions described earlier. Samples were processed in situ on elastic membranes. Immunohistochemistry of cultured neonatal myocytes was performed as previously described (Wang et al., 1998). Cells were washed with PBS and fixed in 4% formaldehyde solution in PBS for 10 min at room temperature. Cells were again washed with PBS and permeabilized with 0.1% Triton X-100 (Sigma) for 10 min, and then washed three times with PBS. The membranes were removed from the stretchers and attached to microscopy slides in the unstretched state. Actin filaments were stained with rhodamine-conjugated phalloidin (Sigma). Intercalated disk proteins, *N*-cadherin and connexin-43, were visualized by the immunohistochemical staining with primary antibodies of monoclonal mouse anti-*N*-cadherin (Zymed Laboratories, Inc.) and rabbit anti-connexin-43 (Zymed). Flourescein isothiocyanate (FITC)-conjugated secondary antibodies raised in mouse and rabbit were used to identify *N*-cadherin and connexin-43, respectively. Immunofluorescent visualization of hypertrophic marker atrial natriuretic

factor (ANF) was carried out with rabbit anti-ANF (Peninsula Laboratories, Inc.) and FITC-conjugated secondary antibody (Sigma). Laser scanning confocal microscopic analysis was performed with a Bio-Rad MRC1024 apparatus, with an identical amplifier and gain setting for each different strain.

Cell Lysate

Anisotropically and statically stretched neonatal cardiac myocytes were washed twice in ice-cold PBS and homogenized with 200 μL of lysis buffer containing ice-cold PBS, 5 m*M* ethylene-diamine tetraacetic acid (EDTA), 1 m*M* phenylmethylsulfonylfluoride, 1 m*M* sodium orthovanadate, and 10 m*M* sodium fluoride. Myocyte lysates were centrifuged at 10,000*g* for 10 min at 4°C, and the pellet was resuspended in 50 μL of lysis buffer and 50 μL of sample buffer containing 37% deionized water, 13% 0.5 *M* Tris-HCl (pH 6.8), 26% glycerol, 21% to 10% sodium dodecylsulfate, and 2% 0.5% (w/v) bromophenol blue.

Total protein concentration was determined with a detergent-compatible protein assay kit (Bio-Rad Laboratories) using bovine gammaglobulin as a standard. Absorbance was measured at 650 nm with a microplate reader (SpectraMAX). Before performing western blotting, β-mercaptoethanol was added to the cell lysate at a 1:20 dilution.

Western Blot Analysis

Cell lysate (25 μL) was resolved by polyacrylamide gel (Ready Gels, Bio-Rad Laboratories) electrophoresis, and the proteins were transferred to nitrocellulose membranes (Bio-Rad). The membrane was blocked for 1 h using 5% milk in TBST buffer (10 m*M* Tris, 0.1 *M* NaCl, 10% Tween 20, pH 7.4). Blots were incubated with the primary antibodies in 5% milk in TBST buffer overnight at 4°C with light agitation. The following primary antibodies were used: monoclonal antibody for actin (Sigma); polyclonal antibody for Cx-43 and monoclonal antibody for *N*-cadherin (Zymed Laboratories); and antibody for ANF. Following the incubation with primary antibodies, blots were washed three times for 10 min each with TBST buffer and then incubated with appropriate horseradish peroxidase-labeled secondary antibodies (Bio-Rad) for 1 h at room temperature, and washed again as indicated earlier. Enhanced chemiluminescence (Pierce Corp.) was employed to detect bound secondary antibodies. Densitometric quantitation of protein bands was performed digitally with CHEMIIMAGER software.

RESULTS

Type I Collagen Micropatterning and Cell Adhesion

High-resolution microscopic observation of collagen micropatterns on silicone elastomers showed discontinuous patterns of collagen deposition in channels with the high and low concentrations of collagen solution used, regardless of the width of the channels, whereas 1000 μg/mL collagen solution produced a regular pattern of collagen adsorption within the channels. Radiolabeling showed that collagen I adsorption increased with increasing solution concentration by reaching about 80% of maximal density (20 $\mu g/cm^2$) near 1000 μg/mL solution (Fig. 5).

Figure 5 also shows myocyte adhesion as a function of matrix concentration. The percentage of cell adhesion to collagen I microchannels was maximal near 1000 μg/mL collagen solution (20 $\mu g/cm^2$ surface density). Light microscopy observation showed the best confluent cell patterns for channels of collagen concentration at between 500 and 2000 μg/mL. Cell shape also varied with concentration of collagen in the microchannels. Polygonal or stellate morphology was observed with lower concentrations of collagen, whereas cells acquired an elongated shape with higher concentrations (1000 to 3000 μg/mL).

Myocyte Morphology

Cells adhered preferentially to collagen-coated microchannels, and by 24 h cells were not observed in the spaces between channels. In the narrowest channels (10 to 30 μm), there was a parallel arrangement of cells along the axis of the channels. In wider channels (>40 μm), cells near the edge of the pattern had a more rod-like, aligned morphology, whereas those near the center of the channel were more irregular and randomly aligned (Fig. 6). There was no significant overlap of myocytes as judged by microscopic observation.

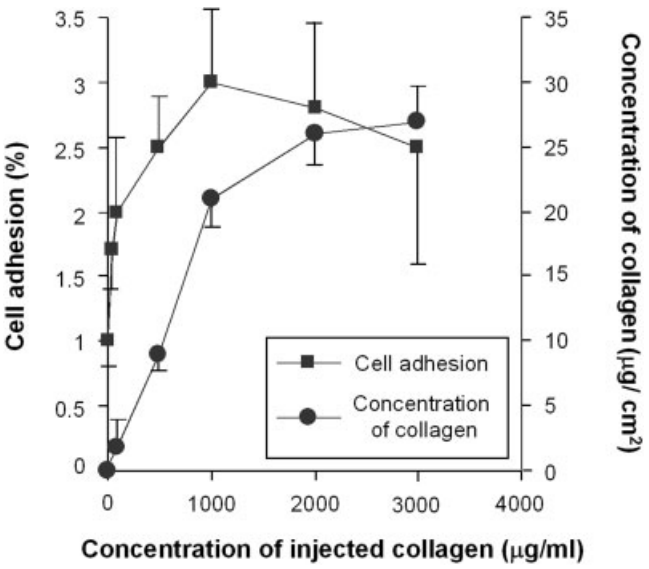

Figure 5. Changes in cell adhesion and collagen concentration adsorbed as functions of collagen concentration infused into the mold (n = 3). Collagen absorbance to the silicone elastomers increases with increase in concentration and starts to plateau near 1000 μg/mL collagen concentration. Maximal cell adhesion also shown to occur at about the same infused collagen concentration (1000 μg/mL).

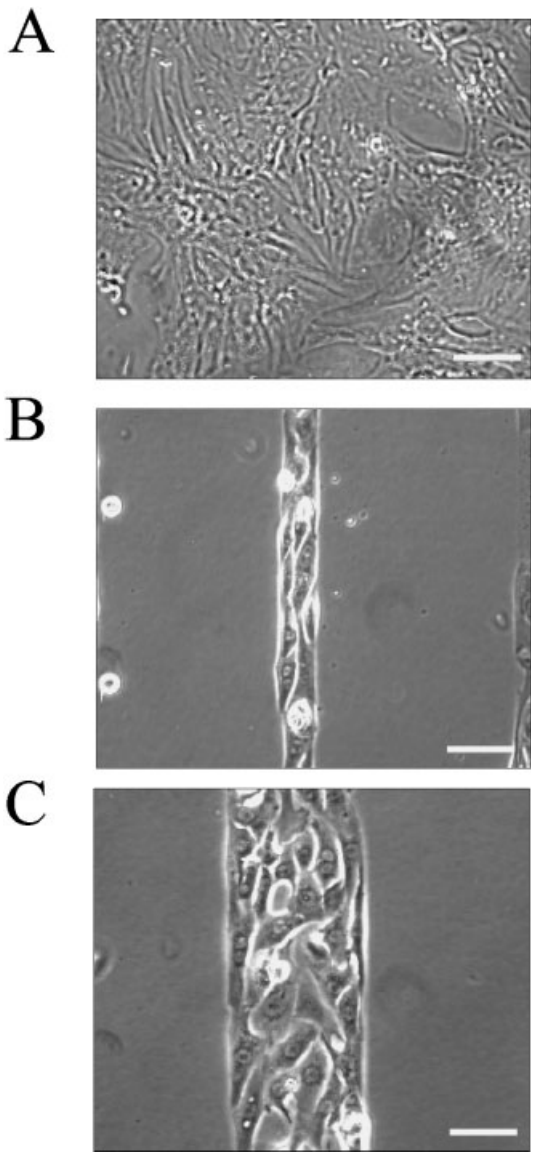

Figure 6. Light micrographs (40×) of neonatal cardiac myocytes grown on: (A) collagen-coated Si elastomers without patterning; (B) 30-μm-width collagen patterns; and (C) 90-μm-width collagen patterns. At widths of >40 μm, no specific orientation of the cells is observed, whereas with the narrower patterns, cells align with the underlying pattern and take on a rod-like phenotype. Scale bars = 50 μm.

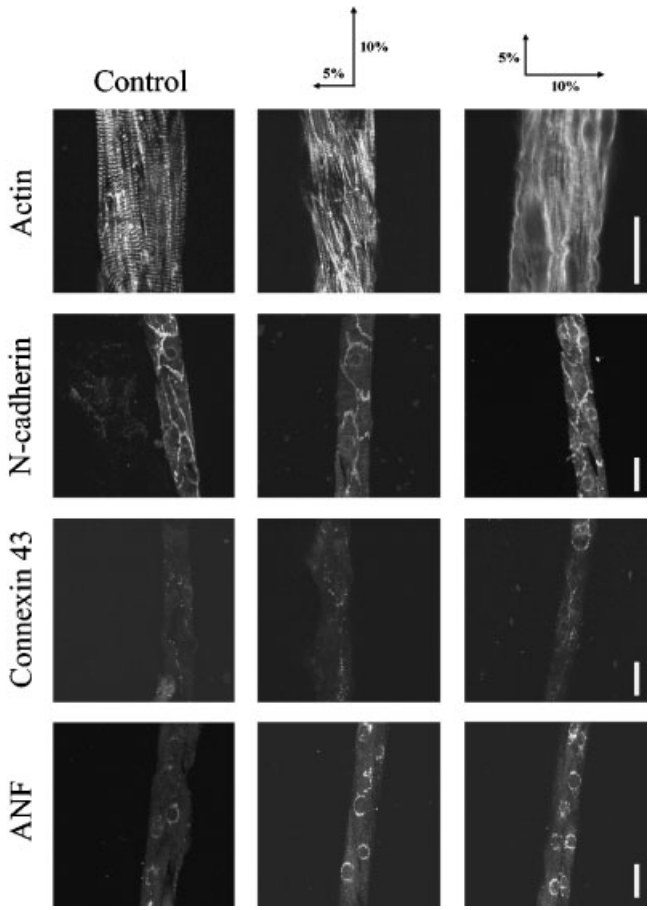

Figure 7. Representative confocal images of aligned myocytes stained for F-actin, *N*-cadherin, connexin-43, and ANF. Each column represents one of three stretch states: no stretch; 10% longitudinal stretch; and 10% transverse stretch. The direction of stretch relative to the cell axis appears to have an effect on protein upregulation. Ten percent transverse stretch shows continuous staining for F-actin, whereas longitudinal stretch does not. Transverse stretching appeared to increase gap junction protein connexin-43 staining, and also the intensity of ANF staining. Scale bar is 30 μm for each label type.

Stretch Responses

Alignment of microchannels with the major axis of the elliptical indenter allowed us to apply maximum principal strain (10%) transverse to the long axis of the cells and minimum principal strain (5%) parallel to the myocyte axis. Myocyte alignment along the minor short axis of the ellipse resulted in maximum principal strain (10%) applied parallel to the myofibers. Figure 7 shows patterned myocytes with four different stains and three stretch states fixed on day 4 of plating. F-actin organization in myocytes stained with rhodamine phalloidin shows aligned myocytes exhibiting a rod-like morphology with polarized arrays of myofibrils and clear I-bands in unstretched controls. Anisotropic stretch with principal strain parallel to the long axis of the cells (longitudinal) did not alter the cell alignment or the pattern of actin staining, whereas cells stretched principally transverse to the myofibers exhibited large regions of intense continuous staining and a loss of striations. Immunoreactive signals of *N*-cadherin appeared as a continuous pattern throughout the cell-to-cell junctions in patterned myocytes with and without stretch. However, upregulation of *N*-cadherin was seen in cells stretched principally transverse to the cell axis, but not longitudinally. Representative confocal images of Cx-43 immunohistochemical staining showed gap junctions in micropatterned neonatal myocytes dotted around the cells predominantly at the ends but also on the sides. Although longitudinal stretching did not significantly alter the intensity or distribution of the Cx-43 immunoreactive signal, there was a marked increase in Cx-43 immunolabeling when principal strain was applied transverse to the myofibers. The mean size of gap junctions appeared to in-

crease and continuous staining of connexin was observed throughout the periphery of the cell. In cells stained for ANF, principal strain applied transverse the myofibrils markedly upregulated ANF expression compared with unstretched controls and longitudinally stretched myocytes. Longitudinally stretched cells did display increased ANF staining in the perinuclear region.

Western blot analysis showed that 24 h of static and anisotropic stretch induced a differential upregulation of actin, connexin-43, *N*-cadherin, and atrial natriuretic factor compared with unstretched controls (Fig. 8). For all four proteins, transverse stretch produced the greater response as compared with longitudinal stretch. As expected, the amount of ANF was greatly increased with stretch, in this case to a greater degree with transverse stretch. In general, these results correlated with immunohistochemical staining.

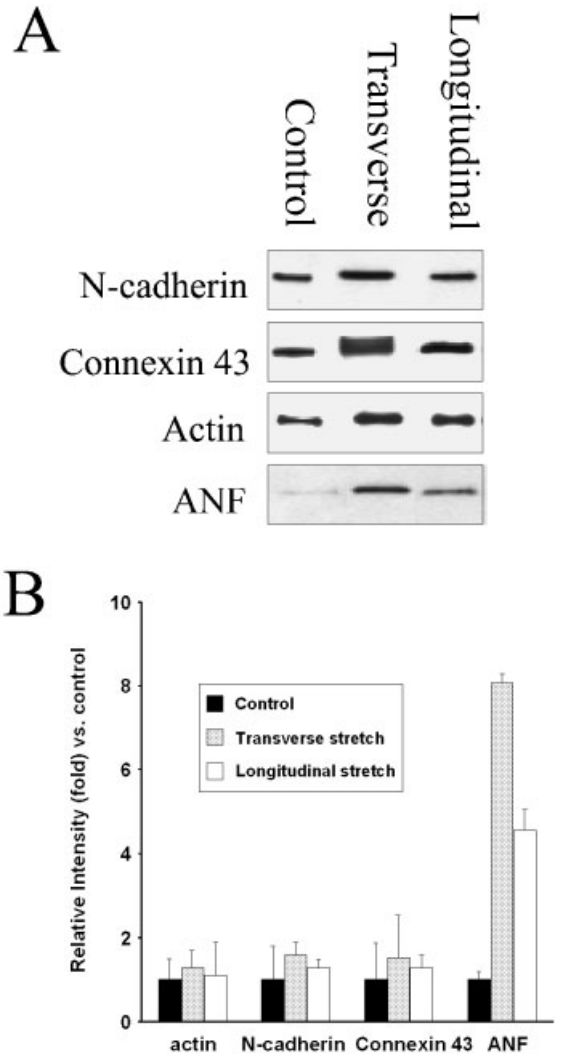

Figure 8. Typical western blot analysis shows the regulation of actin, *N*-cadherin, connexin-43, and ANF with 24-h static anisotropic stretch, and in general correlates with immunohistochemistry. (B) Relative intensity of immunoblots vs. control (mean ± SD; n = 6). Transverse stretch (across the long axis of the cell) shows greater increases in protein content compared with longitudinal stretch.

DISCUSSION

Ventricular myocytes in intact myocardium have a characteristic rod-shaped morphology and are organized by the collagen extracellular matrix into a fibrous architecture. In cell culture, they lose responsiveness to hypertrophic stimuli and become more pleiomorphic (Guo et al., 1986). Therefore, use of neonatal myocytes is the preferred in vitro model system for investigating myocyte hypertrophy. Studies have shown that mechanical stretch as well, as agonists, can stimulate gene expression (Komuro et al., 1991), protein metabolism, and myofibrillar organization (Simpson et al., 1996) in cultured neonatal cardiac myocytes, or even, if the stretch is too great, apoptosis (Cheng et al., 1995).

However, isolated neonatal cardiac myocytes also lack an in vivo morphology and tissue organization when grown in culture. Controlling extracellular matrix composition and spatial distribution has been shown to influence cell phenotype in many cell types. Simpson et al. (1994b) demonstrated that promoting collagen fibrils to polymerize in long parallel arrays on the culture substrate modified the myocyte phenotype, giving rise to elongated rod-shaped cells. Using this technique, they subsequently showed that specific directions and magnitudes of stretch regulate myofibrillar protein accumulation, contractile protein turnover, and sarcomere structure in cultured myocytes (Simpson et al., 1999). Uniaxial stretch, transverse to the myofiber axis suppressed contractile protein turnover in pulse–chase experiments, thus enhancing myofibrillar accumulation, whereas stretch parallel with the myocytes had no effect on protein turnover. These results are consistent with our own observations. By applying a more physiological biaxial stretch, we observed hypertrophic responses, which appeared to be greater with transverse stretch. These differences may contribute to different patterns of cell growth in vivo, such as eccentric vs. concentric hypertrophy (Calderone et al., 1995; Simpson et al., 1995), or to regional differences in myocyte hypertrophy (Omens and Covell, 1991).

Cell–matrix interactions have also been strongly implicated in mechanical signal transduction. For example, activation of extracellular signal-regulated kinase (ERK) and c-Jun NH_2-terminal kinase (JNK) by biaxial mechanical stretch in adult cardiac fibroblasts has been shown to be matrix-specific and integrin-dependent (MacKenna et al., 1998). McKenna and co-workers also emphasized the importance of controlling for cell adhesion in studies of mechanical signaling, because cell phenotype and the force transmitted from substrate to cell are both adhesion-dependent. Finally, cell–cell interactions may also influence the cell response to external loading and are themselves affected by mechanical loading. In isolated neonatal cardiac myocytes, Cx-43 expression, gap junction formation, and action potential propagation velocity increase within hours of the onset of stretch (Zhuang et al., 2000).

Based on these findings, we sought to develop a system in which isolated neonatal cardiac myocytes could be grown

on deformable elastic substrata under conditions in which cell shape and alignment, cell–cell contact and cell–matrix adhesion, and extracellular matrix composition and concentration could be controlled independently. This would allow the effects of cell–matrix interactions and cell–cell contact on myocyte responses to anisotropic multiaxial strains to be investigated while controlling for cell shape and adhesion (MacKenna et al., 1998; Mooney et al., 1995). Photolithography and micropatterning of self-assembled monolayers have been used for spatially organizing proteins and cells. Unfortunately, photolithography is classically limited to rigid materials. Alternative approaches for cell micropatterning include thermosensitive polymers (Ito et al., 1997), protein irradiation (Letourneau, 1975), laminar flow patterning, microcontact printing with elastomeric stamps, and capillary micromolding (Gombotz et al., 1991). Folch et al. (1999) used microfluidic channels to pattern cells on biocompatible substrates. They created protein templates on surfaces by adsorption from solutions that flowed through elastomeric microchannels. Microfluidic access was achieved through a post fixed at the inlet of each channel. We have adapted this method to pattern neonatal myocytes on a silicone membrane fixed to an anisotropic homogeneous cell stretcher. We fabricated an elastomeric master that has a planar surface with a network of microchannels by casting PDMS against a complementary relief structure. Microchannels were perfused continuously with 1000 μg/mL of type I collagen by applying suction, which allowed for precise control over the rate of collagen flow.

To prevent cell adhesion between matrix-coated microchannels, we used Pluronic F108, which is thought to undergo irreversible adsorption to hydrophobic materials, such as silicone, via its hydrophobic polypropylene core. The polyethylene oxide tails are well known for their ability to form a barrier to reduce nonspecific adsorption of adhesive proteins (Lee et al., 1990; Neff et al., 1999). Using this technique, Liu et al. (2002) showed that murine fibroblasts micropatterned on tissue-culture polystyrene retained their pattern fidelity for up to 28 days in the presence of 10% serum.

It is important to control for cell–matrix adhesion in studies of stretch signaling, and extracellular matrix concentration can also influence cell spreading, shape, and phenotype. The amount of collagen adsorbed to the silicone membranes increased as the concentration of collagen in solution was increased up to 1000 μg/mL, above which the collagen adsorbed began to saturate. The resulting protein surface density was 30- to 35-$\mu g/cm^2$ type I collagen, the same as that achieved by passive adsorption into unpatterned silicone membranes at this concentration of collagen solution. At this surface density of collagen, adhesion of neonatal myocytes to patterned microchannels was maximal, and myocytes became mostly elongated and rod-like, as compared with lower concentrations where they were more polygonal. Less efficient adhesion at higher concentrations may be associated with a less homogeneous surface coating. Scanning electron microscopy showed that collagen microfibrils were less uniform and parallel and more discontinuous at higher and lower concentrations. The ability of cells to bind to surface-bound collagen is affected by both the orientation and conformation of the collagen on the surface relative to its receptor binding (Neff et al., 1999).

The replication molding approach allows geometric variables such as collagen width and separation to be controlled independently. We kept channels >100 μm apart in these studies, because closer channel separations have been associated with the occasional appearance of individual myocytes forming transverse bridges spanning adjacent channels. Microchannel width had a profound effect on cell morphology. In channels 10 μm wide, cells were highly elongated, and aligned in single file. At 30-μm width, cells were still rod-shaped, but with room to permit side-to-side as well as end-to-end cell–cell contact. In yet wider channels, myocytes tended to remain elongated and aligned at the edges of the microchannels; however, near the center, alignment sometimes became more random and cells were more irregular in shape. Therefore, for type I collagen matrix and neonatal cardiac myocytes maintained in this culture system, we chose an optimal microchannel width of 30 μm. This gave rise to repeatable rod-shaped myocytes aligned in parallel with end-to-end and side-to-side cell contact.

Myocyte deformations in vivo are multiaxial and anisotropic. For example, during passive loading there are differences in fiber vs. cross-fiber stretch (Omens et al., 1991) with fiber stretch tending to be greater than that of cross-fiber. Similar differences have been seen in systolic deformations (Waldman et al., 1985). Differential responses to chronic fiber vs. cross-fiber loading may contribute to regional variations in cell growth reported in hypertrophy models in vivo (Omens and Covell, 1991). By aligning collagen microchannels with the major or minor axis of the elliptical cell stretchers, the effects of anisotropic strains could be examined in vitro, and stretch similar to that seen in the intact heart can be duplicated. Cells arrayed in parallel to the 10% principal strain did not display altered actin filament organization, gap junction protein distribution, or ANF expression. In contrast, the same magnitude of principal stretch applied across the short axis of the cells significantly altered actin filament organization and increased expression of Cx-43, *N*-cadherin, and ANF. With 10% principal stretch along the long axis of the cell, there appeared to be altered organization of the I-bands, and some inconsistent decrease in the I-band spacing. In general, there appeared to be disruption of the normal actin structure with this type of stretch. Further studies are needed to examine the mechanism behind this response. Long-term pressure and volume overload have been shown to result in morphologically and functionally distinct forms of myocardial hypertrophy (Calderone et al., 1995). The cellular mechanism behind these different responses is not known. Perhaps the direction of stretch is one way that myocytes can distinguish different types of loads, in theory responding with different modes of growth (Sugden, 2001). The observed changes in

myofibrillar organization and ANF expression with stretch are also consistent with the activation of Rho (Hoshijima et al., 1998).

Anisotropic stretch of myocytes with principal strain across the long axis of cells produced marked upregulation of Cx-43 and *N*-cadherin in intercellular junctions after 24 h. Previous studies have shown that expression of Cx-43 and other gap junction proteins is induced by early mediators of hypertrophy, such as cAMP (Darrow et al., 1996) and angiotensin II (Dodge et al., 1998). Although upregulation of Cx-43 expression and a marked increase in gap junction number were prominent features in cells subjected to principal strain across the myofibers, 10% longitudinal stretch had little effect. Thus principal stretch across the myofibers and stretch along the myofibers may activate different mechanotransduction signaling pathways. The mechanism behind differential production of intercellular junction proteins is not known, nor it is clear whether accumulation of protein in intercellular junctions is due to increased synthesis, decreased degradation, enhanced translocation of intracellular protein to cell surface junctions, or a combination of these processes.

In general, immunoblot data correlate with immunohistochemistry for actin, Cx-43, *N*-cadherin, and ANF with 24-h anisotropic stretch. The increase in Cx-43 with 10% transverse strain may indicate increased cell–cell communication with this type of growth stimulus. ANF is a well-known marker of hypertrophy and is upregulated with stretch of myocytes. These results suggest that this response may be direction-dependent, with a much greater hypertrophic response when myocytes are stretched across their long axis.

We did not measure the protein activation with anisotropic stretch for shorter time periods. However, we postulate that temporal differences in the activation of proteins may be due to stimulation of different signaling pathways that are involved in myocardial remodeling. The mechanisms responsible for the distinct patterns and time courses of protein upregulation remain to be defined.

In summary, the new combination of soft lithographic and microfluidic techniques described herein allows cells to be grown on deformable substrata with a much greater degree of spatial and directional control over matrix composition, cell morphology, cell–cell contact, and cell–matrix adhesion than has previously been possible. By micropatterning silicone elastomers with extracellular matrix proteins, neonatal cardiac myocytes were more confluent, aligned, and rod-shaped, consistent with a more adult-like phenotype than conventional cardiac myocyte cell cultures. Control over the chemistry of surface collagen grafting on silicone elastomers further improves the reproducibility of the cell cultures. By aligning myocytes on elastic substrata, we observed differential responses to anisotropic strain the using a new homogeneous cell stretch device. In general, 10%:5% biaxial strain had a significantly more pronounced hypertrophic effect when the direction of maximum strain was transverse to the myofiber axis than when it was parallel to the myofilaments. This may be associated with the spatial distribution of receptors, the orientation of cytoskeletal structures, or some other factor. Elucidating the structural role of these protein activation pathways may lead to a better understanding of the mechanisms behind pathological cellular hypertrophy.

The authors gratefully acknowledge the technical assistance of Keith Herrmann, Zhuangjie Li, and Ned Jastromb in the experimental studies.

References

Anversa P, Ricci R, Olivetti G. 1986. Quantitative structural analysis of the myocardium during physiologic growth and induced cardiac hypertrophy: a review. J Am Coll Cardiol 7:1140–11149.

Bhatia SN, Yarmush ML, Toner M. 1998. Micropatterning cells in tissue engineering. In: Methods in molecular medicine. Totowa, NJ: Humana Press.

Bhatia SN, Balis UJ, Yarmush ML, Toner M. 1999. Effect of cell–cell interactions in preservation of cellular phenotype: cocultivation of hepatocytes and nonparenchymal cells. FASEB J 13:1883–1900.

Bhatia SN, Yarmush ML, Toner M. 1997. Controlling cell interactions by micropatterning in co-cultures: hepatocytes and 3T3 fibroblasts. J Biomed Mater Res 34:189–199.

Borg TK, Rubin K, Lundgren E, Borg K, Obrink B. 1984. Recognition of extracellular matrix components by neonatal and adult cardiac myocytes. Dev Biol 104:86–96.

Calderone A, Takahashi N, Izzo NJ Jr, Thaik CM, Colucci WS. 1995. Pressure- and volume-induced left ventricular hypertrophies are associated with distinct myocyte phenotypes and differential induction of peptide growth factor mRNAs. Circulation 92:2385–2390.

Chandy T, Sharma CP. 1986. Protein/platelet interaction with an artificial surface: effect of vitamins and platelet inhibitors. Thromb Res 41: 9–22.

Chen G, Ito Y, Imanishi A, Magnani S, Lamponi R, Barbucci M. 1997. Photoimmobilization of sulfated hyaluronic acid for antithrombogenicity. Bioconj Chem 85:730–734.

Cheng W, Li B, Kajstura J, Li P, Wolin MS, Sonnenblick EH, Hintze TH, Olivetti G, Anversa P. 1995. Stretch-induced programmed myocyte cell death. J Clin Invest 96:2247–2259.

Darrow BJ, Fast VG, Kleber AG, Beyer EC, Saffitz JE. 1996. Functional and structural assessment of intercellular communication. Increased conduction velocity and enhanced connexin expression in dibutyryl cAMP-treated cultured cardiac myocytes. Circ Res 79:174–183.

Delamarche E, Bernard A, Schmid H, Michel B, Biebuyck H. 1997. Patterned delivery of immunoglobulins to surfaces using microfluidic networks. Science 276:779–781.

Desai TA, Hansford DJ, Ferrari M. 2000. Micromachined interfaces: new approaches in cell immunoisolation and biomolecular separation. Biomol Eng 17:23–36.

Deutsch J, Motlagh D, Russell B, Desai TA. 2000. Fabrication of microtextured membranes for cardiac myocyte attachment and orientation. J Biomed Mater Res 53:267–275.

Dodge SM, Beardslee MA, Darrow BJ, Green KG, Beyer EC, Saffitz JE. 1998. Effects of angiotensin II on expression of the gap junction channel protein connexin43 in neonatal rat ventricular myocytes. J Am Coll Cardiol 32:800–807.

Folch A, Ayon A, Hurtado O, Schmidt MA, Toner M. 1999. Molding of deep polydimethylsiloxane microstructures for microfluidics and biological applications. J Biomech Eng 121:28–34.

Gombotz WR, Guanghui W, Horbert TA, Hoffman AS. 1991. Protein adsorption to poly(ethylene oxide) surfaces. J Biomed Polym Res 25: 1547–1562.

Guo J-X Jacobson SL, Brown DL. 1986. Rearrangement of tubulin, actin

and myosin in cultured ventricular cardiomyocytes of the adult rat. Cell Motil Cytoskel 6:291–304.

Hoshijima M, Sah VP, Wang Y, Chien KR, Brown JH. 1998. The low molecular weight GTPase Rho regulates myofibril formation and organization in neonatal rat ventricular myocytes. Involvement of Rho kinase. J Biol Chem 273:7725–7730.

Ito Y, Chen GP, Guan YQ, Imanishi Y. 1997. Patterned immobilization of thermoresponsive polymer. Langmuir 13:2756.

Iwaki K, Sukhatme VP, Shubeita HE, Chien KR. 1990. Alpha- and beta-adrenergic stimulation induces distinct patterns of immediate early gene expression in neonatal rat myocardial cells. fos/jun expression is associated with sarcomere assembly; Egr-1 induction is primarily an alpha1-mediated response. J Biol Chem 265:13809–13817.

Jo S, Park K. 2000. Surface modification using silanated poly(ethylene glycol)s. Biomaterials 21:605–616.

Komuro I, Katoh Y, Kaida T, Shibazaki Y, Kurabayashi M, Hoe E, Takaku F, Yazaki Y. 1991. Mechanical loading stimulates cell hypertrophy and specific gene expression in cultured rat cardiac myocytes. Possible role of protein kinase C activation. J Biol Chem 266.

Lee AA, Delhaas T, Waldman LK, MacKenna DA, Villarreal FJ, McCulloch AD. 1996. An equibiaxial strain system for cultured cells. Am J Physiol 271:C1400–C1408.

Lee JH, Kopeckova P, Kopecek J, Andrade JD. 1990. Surface properties of alkyl methacrylate with methoxy(polyethylene oxide) methacrylates and their application as protein-resistant coatings. Biomaterials 11: 455–463.

Letourneau PC. 1975. Cell-to substratum adhesion and guidance of axonal elongation. Dev Biol 44:92–101.

Liu VA, Jastromb WE, Bhatia, SN. 2002. Engineering protein and cell adhesivity using PEO- terminated triblock polymers. J Biomed Mater Res 60:126–134

Lom B, Healy KE, Hockberger PE. 1993. A versatile technique for patterning biomolecules onto glass coverslips. J Neurosci Meth 50: 385–397.

MacKenna DA, Dolfi F, Vuori K, Ruoslahti E. 1998. Extracellular signal-regulated kinase and c-Jun NH2-terminal kinase activation by mechanical stretch is integrin-dependent and matrix- specific in rat cardiac fibroblasts. J Clin Invest 101:301–310.

Mooney DJ, Langer R, Ingber DE. 1995. Cytoskeletal filament assembly and the control of cell spreading and function by extracellular matrix. J Cell Sci 108:2311–2320.

Neff JA, Tresco PA, Caldwell KD. 1999. Surface modification for controlled studies of cell–ligand interactions. Biomaterials 20:2377–2393.

Omens JH, Covell JW. 1991. Transmural distribution of myocardial tissue growth induced by volume- overload hypertrophy in the dog. Circulation 84:1235–1245.

Omens JH, May KD, McCulloch AD. 1991. Transmural distribution of three-dimensional strain in the isolated arrested canine left ventricle. Am J Physiol 261:H918–H928.

Rohr S, Scholly DM, Kleber AG. 1991. Patterned growth of neonatal rat heart cells in culture. Morphological and electrophysiological characterization. Circ Res 68:114–130.

Sadoshima J, Izumo S. 1993. Mechanotransduction in stretch-induced hypertrophy of cardiac myocytes. J Recept Res 13:777–794.

Simpson DG, Carver W, Borg TK, Terracio L. 1994a. Role of mechanical stimulation in the establishment and maintenance of muscle cell differentiation. Int Rev Cytol 150:69–94.

Simpson DG, Terracio L, Terracio M, Price RL, Turner DC, Borg TK. 1994b. Modulation of cardiac myocyte phenotype in vitro by the composition and orientation of the extracellular matrix. J Cell Physiol 161:89–105.

Simpson DG, Majeski M, Borg TK, Terracio L. 1999. Regulation of cardiac myocyte protein turnover and myofibrillar structure in vitro by specific directions of stretch. Circ Res 85:E59–E69.

Simpson DG, Sharp WW, Borg TK, Price RL, Samarel AM, Terracio L. 1995. Mechanical regulation of cardiac myofibrillar structure. Ann NY Acad Sci 752:131–140.

Simpson DG, Sharp WW, Borg TK, Price RL, Terracio L, Samarel AM. 1996. Mechanical regulation of cardiac myocyte protein turnover and myofibrillar structure. Am J Physiol 270:C1075–C1087.

Sugden PH. 2001. Mechanotransduction in cardiomyocyte hypertrophy. Circulation 103:1375–1377.

Summerour SR, Emery JL, Fazeli B, Omens JH, McCulloch AD. 1998. Residual strain in ischemic ventricular myocardium. J Biomech Eng 120:710–714.

Uniyl S, Brash JL. 1982. Patterns of adsorption of proteins from human plasma on to foreign surfaces. Thromb Haemostas 47:285–290.

Waldman LK, Fung YC, Covell JW. 1985. Transmural myocardial deformation in the canine left ventricle: normal in vivo three-dimensional finite strains. Circ Res 57:152–163.

Wang N, Ingber DE. 1994. Control of cytoskeletal mechanics by extracellular matrix, cell shape, and mechanical tension. Biophys J 66: 2181–2189.

Wang TL, Tseng YZ, Chang H. 2000. Regulation of connexin 43 gene expression by cyclical mechanical stretch in neonatal rat cardiomyocytes. Biochem Biophys Res Commun 267:551–1557.

Wang Y, Su B, Sah VP, Brown JH, Han J, Chien KR. 1998. Cardiac hypertrophy induced by mitogen-activated protein kinase kinase 7, a specific activator for c-Jun NH_2-terminal kinase in ventricular muscle cells. J Biol Chem 273:5423–5426.

Zhuang J, Yamada KA, Saffitz JE, Kleber AG. 2000. Pulsatile stretch remodels cell-to-cell communication in cultured myocytes. Circ Res 87:316–322.